British Microbiology Research Journal
4(9): 968-987, 2014

SCIENCEDOMAIN *international*
www.sciencedomain.org

An Analysis of the Electronic Structure of an Imidazo [1,2-*a*] Pyrrolo [2,3-*c*] Pyridine Series and Their Anti-Bovine Viral Diarrhea Virus Activity

Juan S. Gómez-Jeria[1*]

[1]*Quantum Pharmacology Unit, Department of Chemistry, Faculty of Sciences, University of Chile, Las Palmeras 3425, Santiago 7800003, Chile.*

Author's contribution

This whole work was carried out by the author JSGJ.

Original Research Article

Received 18th February 2014
Accepted 4th April 2014
Published 22nd May 2014

ABSTRACT

The aim of this study was to analyze the relationship between electronic structure and anti Bovine Viral Diarrhea Virus activity in a series of imidazo[1,2-*a*] pyrrolo [2,3-*c*]pyridine derivatives. The electronic structure and the local atomic reactivity indices were obtained with density functional theory at the B3LYP/6-31G (d,p) level. A statistically significant equation (n=15, R=0.90, R^2=0.82, adj R^2=0.77, F(3,11)=16.60 ($p<0.0002$), outliers>2σ=0, SD=0.29) relating the variation of the antiviral activity with the variation of the electron-donor and electron-acceptor properties of three atoms was obtained. The variation of antiviral potency is orbital-controlled. A partial antiviral pharmacophore is proposed.

Keywords: Imidazo [1,2-a] pyrrolo [2,3-c] pyridine derivatives; bovine viral diarrhea virus; quantitative structure-activity relationships.

1. INTRODUCTION

Bovine Viral Diarrhea Virus (BVDV) was first recognized as a viral disease in 1946. BVDV is classified in the *Pestivirus* genus within the *Flaviviridae* family, which also contains the *Flavivirus* and *Hepacivirus* genera [1-3]. There are at least two genotypes (BVDV1 and

**Corresponding author: Email: facien03@uchile.cl;*

BVDV2); and two biotypes (cytopathic and noncytopathic). Both BVDV1 and BVDV2 genotypes have cytopathic and noncytopathic biotypes as members; and both BVDV1 and BVDV2 genotypes have many different strains. The virus is distributed worldwide. Domestic cattle seem to be the primary host, and BVDV is considered an economically important pathogen of cattle in most regions of the world (BVDV also infects sheep and other ruminants and pigs [4], but these infections are mainly subclinical) [5-14]. Today, 70 to 90 percent of the world's cattle population is seropositive for BVDV. It can cause a diversity of problems for cattle producers including reduced pregnancy rate, increased abortion, stillbirth, increased calf sickness and loss. An important problem associated with BVDV is the development of persistent infection [5]. In persistent infection an animal is already infected with BVDV when it is born and it remains infected during its whole life. Cattle persistently infected with BVDV are the primary reservoir for BVDV infection in cattle herds, continue to have a heavy economic impact in the cattle industry and thus are the major focus of control programs. Also, it is interesting to mention that BVDV is a good candidate for oncolytic therapies [15]. The BVDV RNA-dependent RNA polymerase (RdRp) can initiate RNA replication by a *de novo* mechanism without a primer. Choi et al. showed that the BVDV NS5B (one of the nonstructural proteins required for viral assembly and replication) binds a guanosine triphosphate (GTP) next to the expected site of the initiation nucleotide and that this extra GTP could provide the initiation platform [16]. Also they showed that BVDV RdRp contains, besides the fingers, palm, and thumb domains common to other polymerases, a unique N-terminal domain. RdRp is then the natural target for antiviral drugs. Neyts et al. analyzed two imidazo [1,2-*a*] pyrrolo [2,3-*c*]pyridine derivatives and concluded that they targeted the top of the finger domain of the RdRp [17]. Recently, Chezal et al reported the synthesis and anti bovine viral diarrhea virus activity of an imidazo [1,2-*a*] pyrrolo [2,3-*c*]pyridine series [18]. As a contribution to the understanding of the molecular action mechanism this paper presents the results of a quantum-chemical study of the relationships between electronic structure and antiviral activity of the abovementioned compounds.

2. METHODS, MODELS AND CALCULATIONS

2.1 The Method

Given that the model-based method relating drug-receptor equilibrium constants with molecular structure has been described in great detail elsewhere, we present here only a standard résumé used in other papers [19-25]. The drug-receptor affinity constant, expressed as K_i, pA_2 or IC_{50}, is a linear function of several local atomic reactivity indices (LARIs) and has the following form:

$$\begin{aligned}\log \mathrm{K}_i = a + bM_{D_i} + c\log\left[\sigma_{D_i}/(ABC)^{1/2}\right] + \sum_j \left[e_j Q_j + f_j S_j^E + s_j S_j^N\right] + \\ + \sum_j \sum_m \left[h_j(m)F_j(m) + x_j(m)S_j^E(m)\right] + \sum_j \sum_{m'} \left[r_j(m')F_j(m') + t_j(m')S_j^N(m')\right] + \\ + \sum_j \left[g_j \mu_j + k_j \eta_j + o_j \omega_j + z_j \varsigma_j + w_j Q_j^{\max}\right] + \sum_{B=1}^{W} O_B \end{aligned} \quad (1)$$

Where M is the drug's mass, σ its symmetry number and ABC the product of the drug's moment of inertia about the three principal axes of rotation. Q_i is the net charge of atom j, S_j^E and S_j^N are, respectively, the total atomic electrophilic and nucleophilic

superdelocalizabilities of Fukui et al. $F_{j,m}$ ($F_{j,m'}$) is the Fukui index of the occupied (vacant) MO m (m') located on atom j [26]. $S_j^E(m)$ is the atomic electrophilic superdelocalizability of MO m on atom j, etc. The total atomic electrophilic superdelocalizability of atom j corresponds to the sum over occupied MOs of the $S_j^E(m)$'s and the total atomic nucleophilic superdelocalizability of atom j is the sum over vacant MOs of the $S_j^N(m)$'s. μ_j is the local atomic electronic chemical potential of atom j, η_j is the local atomic hardness of atom j [27], ω_j is the local atomic electrophilicity of atom j, ς_j is the local atomic softness of atom j, and $Q_j^{\max}$ is the maximal amount of electronic charge that atom j may accept from another site. $HOMO_j$* refers to the highest occupied molecular orbital localized on atom j and $LUMO_j$* to the lowest empty MO localized on atom j. They are called the local atomic frontier MOs. The molecule's MOs do not carry an asterisk. The O_B's are the so-called orientational parameters for the different substituents, and are related to their influence on the fraction of molecules attaining the right orientation to interact with the partner [21,22]. Then, for n molecules, we have a set of n simultaneous equations. Table 1 presents the physical interpretation and units of the LARIs together with the appropriate references [21,22,26-28].

The application of this method to the drug-receptor interaction has been very successful for several systems [21,23,29-43]. For a correct understanding of the results presented below, let us remember that the conceptual bases of this model-based method are found in the works of Agin, Peradejordi, Cammarata and Klopman [44-50]. Equation 1 was obtained from the statistical mechanical definition of the equilibrium constant, K_i:

$$K_i = \frac{Q_{D_iR}}{Q_{D_i} Q_R} \exp(-\Delta\varepsilon_0^i / kT) \tag{2}$$

Where R refers to the receptor, D_i to the drug, D_iR to the drug-receptor complex and $\Delta\varepsilon_0^i$ to the difference between the ground-state energy of D_iR and the energies of the ground states of D_i and R:

$$\Delta\varepsilon_0^i = \varepsilon_{D_iR} - (\varepsilon_{D_i} + \varepsilon_R) \tag{3}$$

The Q's are the corresponding total partition functions. From these last terms we have derived the Orientational parameters (from the rotational partition functions) [22]. The molecular masses come from the translational partition functions [19]. For this specific case we have considered in a first approach that the molecular masses are similar (i.e., for a given temperature the corresponding Boltzmann distributions are quite similar). The other term is $\Delta\varepsilon_0^i$. Usually $\Delta\varepsilon_0^i$ cannot be calculated directly. The first breakthrough was to use perturbation theory (in the Klopman-Hudson form, [45,46,49]) to rewrite $\Delta\varepsilon_0^i$ in terms of local atomic reactivity indices. The second main advance was to use a series expansion to expand the expression of $\Delta\varepsilon_0^i$ in terms of more local atomic reactivity indices [27]. Let us note the important fact that the numerical values of the reactivity indices depend on the

quantum-chemical method to obtain them (for an example of anomalous numerical behavior see [51]). On the other hand, we have recently proposed that *log (K_i)* can be replaced by *log (BA),* where *BA* is any biological activity measured *In vivo* or *In vitro*. This extension was successfully applied to the study of several very different processes [25,52-57]. This replacement will successfully work if and only if all the molecules studied exert their final biological activity through the same mechanism or mechanisms. If this condition is not fulfilled, we cannot expect to obtain good results for the whole set.

Table 1. Local Atomic Reactivity Indices and their physical meaning

LARI	Name	Physical interpretation	Units
Q_i	Net atomic charge of atom i	Electrostatic interaction	e
S_i^E	Total atomic electrophilic superdelocalizability of atom i	Total atomic electron-donating capacity of atom i (MO-MO interaction) [26]	e/H
S_i^N	Total atomic nucleophilic superdelocalizability of atom i	Total atomic electron-accepting capacity of atom i (MO-MO interaction) [26]	e/H
$S_i^E(m)$	Orbital atomic electrophilic superdelocalizability of atom i and occupied MO m	Electron-donating capacity of atom i at occupied MO m (MO-MO interaction) [26]	e/H
$S_i^N(m')$	Orbital atomic nucleophilic superdelocalizability of atom i and empty MO m’	Electron-accepting capacity of atom i at vacant MO m’ (MO-MO interaction) [26]	e/H
F_i	Fukui index of atom i	Total electron population of atom i (MO-MO interaction) [26,28]	e
F_{mi}	Fukui index of atom i and occupied MO m.	Electron population of occupied m MO at atom i (MO-MO interaction) [26,28]	e
$F_{m'i}$	Fukui index of atom i and empty MO m’	Electron population of vacant MO m’ at atom i (MO-MO interaction) [26,28]	e
μ_i	Local atomic electronic chemical potential of atom i	Propensity of atom i to gain or lose electrons. $HOMO_i$*-$LUMO_i$* midpoint [27]	eV
η_i	Local atomic hardness of atom i	Resistance of atom i to exchange electrons with the environment. $HOMO_i$*-$LUMO_i$* gap [27]	eV
ς_i	Local atomic softness of atom i	The inverse of η_i	1/eV
ω_i	Local atomic electrophilicity of atom i	Tendency of atom i to receive extra electronic charge together with its resistance to exchange charge with the medium [27]	eV
$Q_i^{\max}$	Charge capacity	Maximal amount of electronic that charge atom i may receive [27]	---
O_t	Orientational Parameter	Influence the fraction of molecules attaining the correct orientation to interact with a partner [21,22]	uma·$Å^2$

2.2 Selection of the Experimental Data

The first essential requirement to employ a set of experimental values in quantitative structure-activity relationships studies is that they be obtained in a precise manner under nearly identical conditions. The biological activity analyzed in this study is the 50% effective concentration (EC_{50}), defined as the concentration of compound that offered 50% protection of the cells against the virus-induced cytopathic effect in MBDK (Madin Darby Bovine Kidney) cells (see Supp. Mat. of [18]). Cytopathic BVDV induces cytoplasmic vacuolation, detachment from the cell sheet, cell rounding, and death of cells. The cytopathic effect habitually occurs within 2 to 3 days of infection of the cell culture. It is important to notice that the exact antiviral action mechanism of these molecules is unclear. The molecules chosen for this study are shown in Fig. 1 and Table 2, together with the corresponding experimental biological activity.

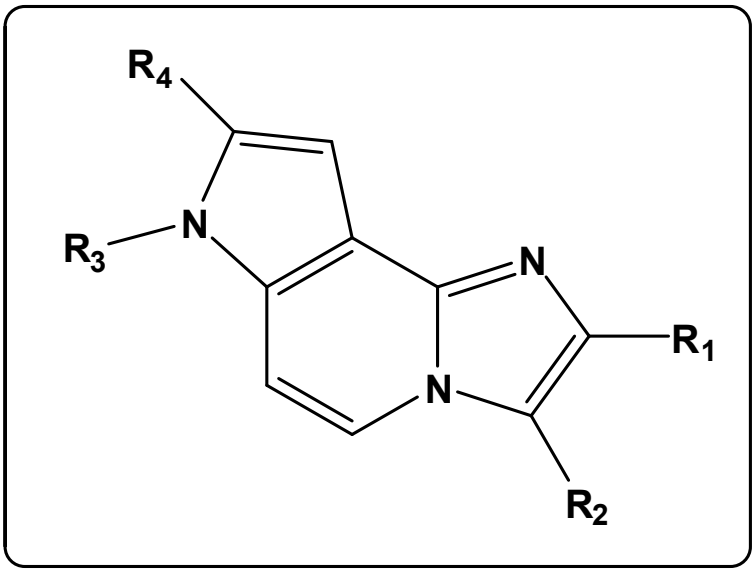

Fig. 1. Imidazo [1,2-*a*] pyrrolo [2,3-*c*] pyridine derivatives

2.3 Calculations

The electronic structure of the molecules was obtained within the Density Functional Theory (DFT) at the B3LYP/6-31g (d,p) level with full geometry optimization. The Gaussian suite of programs was employed [58]. The numerical values for the local atomic reactivity indices were calculated with software written in this Unit. Negative electron populations coming from Mulliken Population Analysis were corrected as suggested [59]. All electron populations smaller than or equal to 0.01 e were considered as zero [27]. Orientational parameters of the substituents were calculated as usual [21,22]. We employed the common skeleton hypothesis: There is a particular set of atoms, common to all molecules analyzed, that accounts for nearly all the biological activity. The variation of the values of a set of local atomic reactivity indices of certain atoms belonging to this skeleton should give an account of the variation of the anti-BVDV activity throughout the series analyzed. The action of the substituents consists in modifying the electronic structure of the common skeleton and influencing the precise alignment of the drug through the orientational parameters. Since the

resolution of the system of n linear equations is not possible because there are not enough cases (molecules), we made use of Linear Multiple Regression Analysis (LMRA) techniques to determine which atoms are directly involved in the variation of the biological activity. We built matrix containing the dependent variable (log (EC_{50})), and the local atomic reactivity indices of all atoms of the common skeleton as independent variables. The Statistica software was used for LMRA [60]. Note that in this study statistics is employed as a servant and not as a queen. The common skeleton numbering is shown in Fig. 2.

Table 2. Imidazo [1, 2-*a*] pyrrolo [2, 3-*c*] pyridine derivatives and their anti-BVDV activity

Mol.	R_1	R_2	R_3	R_4	log(EC_{50}) (µM)
1	H	H	H	CO_2Et	0.70
2	Br	H	H	CO_2Et	1.12
3	Me	H	H	CO_2Et	0.32
4	Ph	H	H	CO_2Et	0.57
5	m-MeOHPh	H	H	CO_2Et	-0.40
6	CF_3	H	H	CO_2Et	1.11
7	*i*-Pr	H	H	CO_2Et	1.36
8	*t*-Bu	H	H	CO_2Et	1.70
9	H	Br	H	CO_2Et	1.15
10	Me	Br	H	CO_2Et	1.90
11	Me	NO_2	H	CO_2Et	1.81
12	$CH(OEt)_2$	H	H	CO_2Et	0.32
13	CHO	H	H	CO_2Et	1.34
14	CH_2OH	H	H	CO_2Et	1.73
15	CH_2Cl	H	H	CO_2Et	1.68
16	$CH_2N(Me)_2$	H	H	CO_2Et	1.67
17	Me	H	H	CO_2H	0.71
18	Me	H	Me	CO_2Me	0.23
18	Me	H	H	CO_2Me	0.04
20	Me	H	H	CO_2Bu	0.32

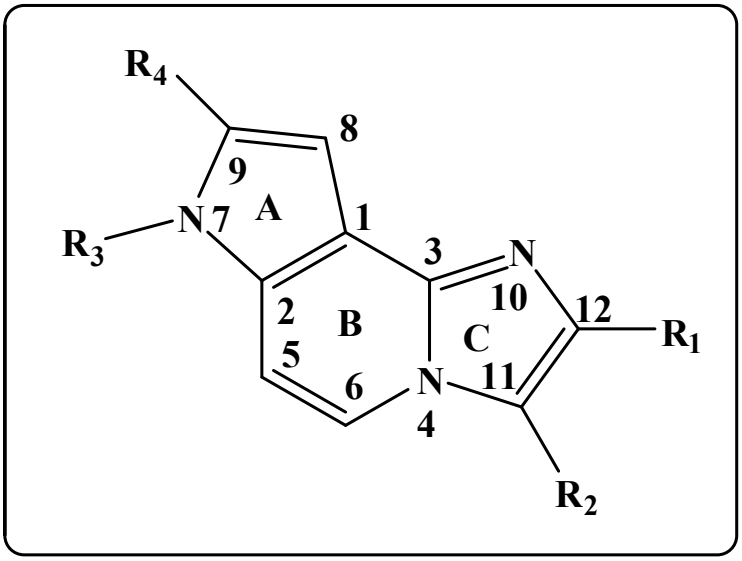

Fig. 2. Common skeleton numbering

3. RESULTS AND DISCUSSION

3.1 Results

A LMRA performed with all the set (n=20) produced no statistically significant equations. We proceeded to test the validity of the common skeleton enlarging it by including the COO moiety. No statistically significant results were obtained. The next step was to consider that the orientational parameters can be employed only in the case in which the molecular skeleton is larger than the substituent. Therefore we included the term $\log\left[1/(ABC)^{1/2}\right]$ of Eq. 1 in the independent variables set. No statistically significant results were obtained (the best equation has adj R^2=0.62 and SD=0.42). Next we turned our attention to the reported experimental values, EC_{50}. In Table 1 it can be seen that they are expressed in μM and that the most active has EC_{50}=0.4 μM and the least active has EC_{50}=78.9 μM. The ratio of these values is about 197. Therefore we tested the hypothesis that molecules presenting a high antiviral activity may exert their action through a different mechanism than those with low activity. First, we carried out a LMRA with the molecules having an EC_{50} in the range 21.8 - 78.9μM (n=8). No statistically significant results were obtained (in the most statistically significant equation there is an unacceptably high degree of correlation between independent variables). Starting from a set including the lowest EC_{50} values and adding molecules with increasing EC_{50} values we obtained the following statistically significant equation for the molecules in the 0.4-47.6 μM range (molecule 7 appeared as an outlier and was discarded):

$$\log(EC_{50}) = 10.0 + 1.81 S_9^E(HOMO-1)^* - 2.75 F_3(LUMO+2)^* + 0.74 S_{12}^E \quad (4)$$

With n=15, R=0.90, R^2=0.82, adj R^2=0.77, F(3,11)=16.60 (*p<0.0002*), outliers>2σ=0 and SD=0.29. Here, S_{12}^E is the total atomic electrophilic superdelocalizability of atom 12 (see Fig. 2), $F_3(LUMO+2)^*$ is the Fukui index (i.e., the electron population) of the third vacant MO localized on atom 3 and $S_9^E(HOMO-1)^*$ is the local electrophilic superdelocalizability of the second highest MO localized on atom 3. The Beta coefficients and t-test for significance of coefficients of Eq. 4 are shown in Table 3. Table 4 shows that, at p<0.05, there are no significant internal correlations between independent variables. Fig. 3 shows the plot of observed values *vs.* calculated ones. The associated statistical parameters indicate that this equation is statistically significant, explaining about the 77% of the variation of the antiviral activity.

Table 3. Beta coefficients and *t*-test for significance of the coefficients in Eq. 4

	Beta	**B**	**t(11)**	***p-level***
$S_9^E(HOMO-1)^*$	0.90	1.81	6.59	<0.00004
$F_3(LUMO+2)^*$	-0.44	-2.75	-3.20	<0.008
S_{12}^E	0.28	0.74	2.10	<0.06

Table 4. Squared correlation coefficients for the variables appearing in Eq. 4

	$S_9^E(HOMO-1)^*$	$F_3(LUMO+2)^*$
$F_3(LUMO+2)^*$	0.11	1.00
S_{12}^E	0.006	0.04

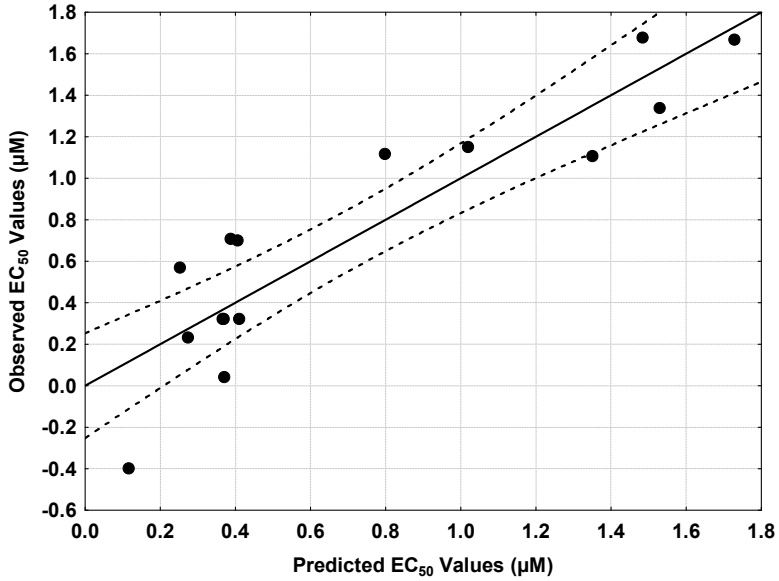

Fig. 3. Observed versus calculated values (Eq. 4) of log (EC_{50}). Dashed lines denote the 95% confidence interval

3.2 Discussion

3.2.1 Molecular electrostatic potential (MEP) of imidazo [1,2-a] pyrrolo [2,3-c] pyridine derivatives

In zone II of Ariëns' model there is an accumulation, recognition and guiding of the drug molecule towards the partner through long-range interactions [20,61]. This recognition process can be associated with the matching of the molecular electrostatic potentials of both partners to generate the correct geometrical alignment before the interaction occurs. Figs. 4 and 5 show, respectively, the MEP of molecules 12 and 3 with an isovalue of ±0.01 [62].

We can see in the upper part of both figures similar large regions of negative MEP. The remaining molecular region has a positive MEP. All the other molecules have a similar MEP structure. The structure of the MEP will vary only slightly with the orientation of the $C(O)OC_2H_5$ fragment. To have an idea of the structure of the MEP at a given distance from the nuclei we present, in Figs. 6 and 7, the MEP of molecules 12 and 3 at 3.5 Å from the nuclei [63].

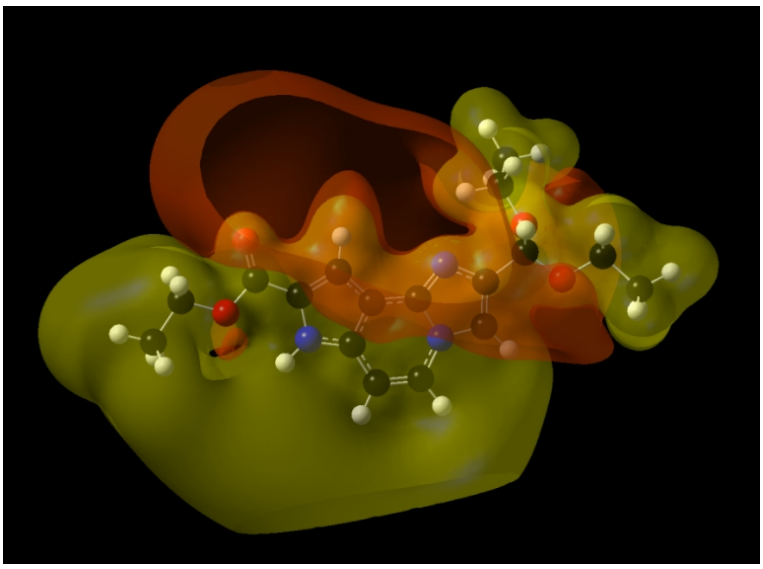

Fig. 4. MEP of molecule 12. The orange isovalue surface corresponds to negative MEP values (-0.01) and the yellow isovalue surface to positive MEP values (0.01)

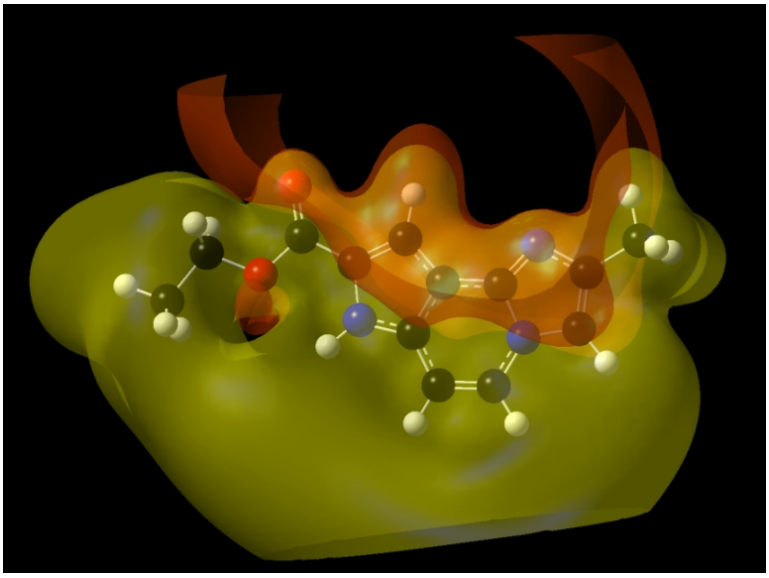

Fig. 5. MEP of molecule 3. The orange isovalue surface corresponds to negative MEP values (-0.01) and the yellow isovalue surface to positive MEP values (0.01)

We can see that the MEP structure of both molecules is similar. If we consider the negative MEP region, in molecule 3 it is more extended (red/yellow/green) than in molecule 12 (red/yellow). A similar MEP structure appears in all the series (not shown here). The negative MEP region probably faces a positive MEP region of the partner. We suggest the existence of a “MEP channel” directing the approach of the molecule towards its partner. The “walls” of this channel should be of negative MEP while in its center the MEP should be

positive. The introduction of the concept of the MEP channel could explain why these molecules bind to these specific kinds of structures and not to others. The X-ray results for drug-receptor complexes (the Protein Data Bank is full of them) may serve to model and test the validity of this concept.

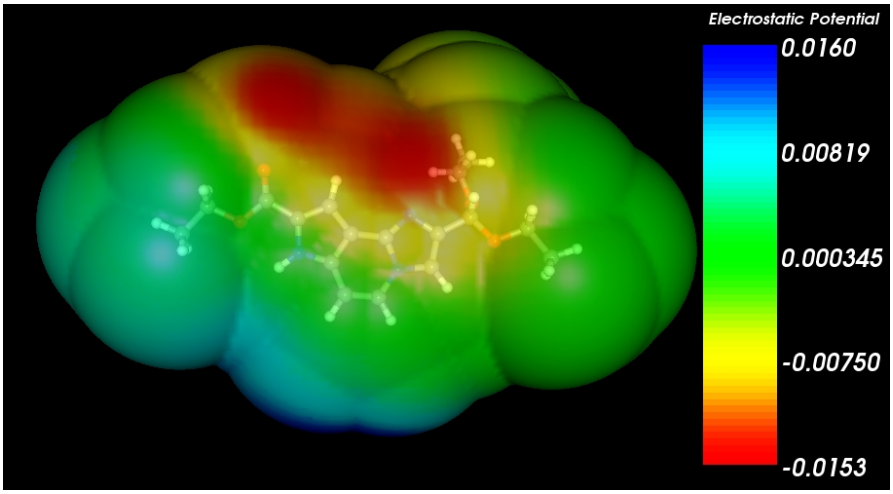

Fig. 6. MEP of molecule 12 at a distance of 3.5 Å from the nuclei

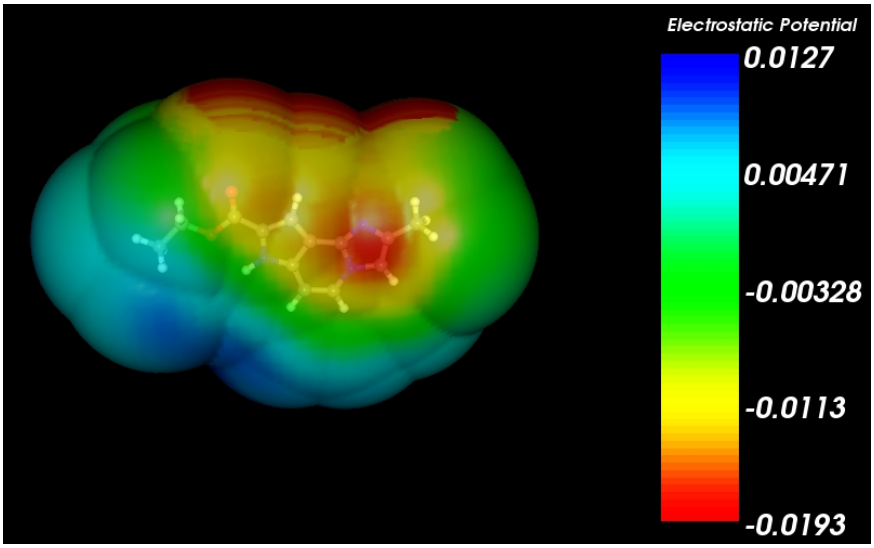

Fig. 7. MEP of molecule 3 at a distance of 3.5 Å from the nuclei

3.2.2 Discussion of the relationship between molecular structure and antiviral activity

Eq. 4 shows that there is a direct dependence of the variation of $\log(EC_{50})$ upon the variation of three local atomic reactivity indices of the common skeleton. The Beta values (Table 3) indicate that the importance of these variables is $S_9^E(HOMO-1)^*$ >> $F_3(LUMO+2)^*$ >> S_{12}^E.

A variable-by-variable analysis of Eq. 4 indicates that strong anti-BVDV activity in MDBK cells is associated with high values of $F_3(LUMO+2)^*$ (rings B/C), and S_{12}^E (ring C), and with low values of $S_9^E(HOMO-1)^*$ (ring A). Table 5 shows the nature of the three highest occupied and three vacant local MOs of atoms 3, 9 and 12 (Nomenclature: Molecule (HOMO) / (HOMO-2)* (HOMO-1)* (HOMO)*-(LUMO)* (LUMO+1)* (LUMO+2)*).

Table 5. Local molecular orbitals of atoms 3, 9 and 12

Mol.	Atom 3 (C)	Atom 9 (C)	Atom 12 (C)
1 (60)	58σ59π60π-61π62π63π	57π59π60π-61π64π65σ	58σ59π60π-61π62π63π
2 (77)	75π76π77π-78π79π80π	75π76π77π-78π83σ84σ	75π76π77π-78π79π80π
3 (64)	62σ63π64π-65π66π67π	61π63π64π-65π68π69σ	62σ63π64π-65π66π67π
4 (80)	77π79π80π-81π82π83π	78π79π80π-81π82π86σ	77π79π80π-81π82π85π
5 (88)	86π87π88π-89π90π91π	85π87π88π-89π90π94σ	86π87π88π-89π90π91π
6 (76)	74σ75π76π-77π78π79π	74σ75π76π-77π78π81σ	74σ75π76π-77π78π79π
7 (72)	70σ71π72π-73π74π75π	69π71π72π-73π76π77σ	70σ71π72π-73π74π75π
8 (76)	74σ75π76π-77π78π79π	73π75π76π-77π80π81σ	74σ75π76π-77π78π79π
9 (77)	75σ76π77π-78π79π80σ	74π76π77π-78π79π82π	75σ76π77π-78π79π80σ
10 (81)	79σ80π81π-82π83π84π	78π80π81π-82π86π87σ	79σ80π81π-82π83π84π
11 (75)	73σ74π75π-76π78π79π	72σ74π75π-76π77π78π	72σ73σ74π-76π78π80π
12 (88)	86σ87π88π-89π90π91π	84π87π88π-89π92π93σ	86σ87π88π-89π90π91π
13 (67)	64π66π67π-68π69π70π	64π66π67π-68π69π72σ	65σ66π67π-68π69π75π
14 (68)	65σ67π68π-69π70π71π	66π67π68π-69π73π74σ	66π67π68π-69π70π71π
15 (72)	70σ71π72π-73π74π75π	70π71π72π-73π74π77σ	70σ71π72π-73π74π75π
16 (76)	74π75π76π-77π78π79π	74π75π76π-77π80π81σ	74π75π76π-77π78π79π
17 (56)	54σ55π56π-57π58π59π	53π55π56π-57π60σ61π	54σ55π56π-57π58π59π
18 (64)	62σ63π64π-65π66π67π	6π163π64π-65π68π70σ	62σ63π64π-65π66π67π
19 (60)	58σ59π60π-61π62π63π	57π59π60π-61π64π65σ	58σ59π60π-61π62π63π
20 (72)	70σ71π72π-73π74π75π	69π71π72π-73π76π77σ	70σ71π72π-73π74π75π

We can see that the (HOMO-1)* has π character in all molecules. Low $S_9^E(HOMO-1)^*$ values can be obtained by lowering the corresponding eigenvalue and/or the associated Fukui index. The only explanation for this requirement is that atom 9 is acting as an electron donor but only through its HOMO*. The partner seems to be constituted by an electron-acceptor center having at least one vacant π MO followed by σ MOs. These σ MOs probably repel the $(HOMO-1)_9$* MO. A high value for $F_3(LUMO+2)^*$, a local π MO in almost all cases, suggests that atom 3 acts as an electron-acceptor site through its three lowest vacant MOs. If this interaction occurs it should be with an electron-rich counterpart. A high value for S_{12}^E is associated with a high electron-donor capability. The total atomic electrophilic superdelocalizability of atom 12 is a sum of $F_{12}(MO)/MO_{energy}$ terms, and the dominant ones correspond to the highest occupied local MOs of atom 12. Then, atom 12 acts as an electron-donor center through, at least, its two highest occupied local MOs. Another possibility is that atoms 3 and 12 participate together in a π-π stacking interaction. These suggestions are depicted in the partial two-dimensional (2D) antiviral pharmacophore depicted in Fig. 8. It must be emphasized that the variation of the antiviral activity is explained by the simultaneous variation of the three indices just discussed. All reactivity indices that do not contribute significantly to the variation of $\log(EC_{50})$ will not explicitly appear in Eq. 4. Note finally that the variation of the antiviral activity is orbital-controlled [59].

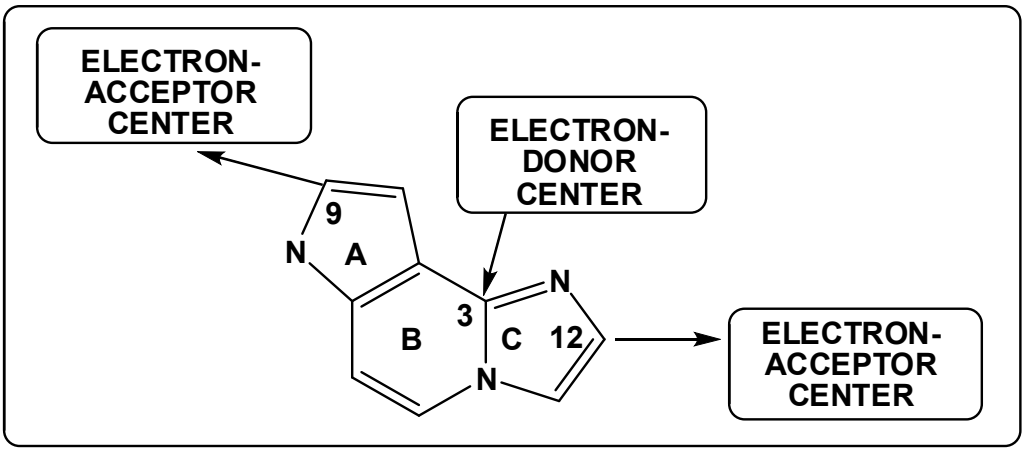

Fig. 8. Partial 2D antiviral pharmacophore

3.2.3 Molecular orbitals of imidazo [1,2-*a*] pyrrolo [2,3-*c*] pyridine derivatives

A qualitative discussion seems necessary prior to the analysis of the MO structure. Within the LCAO-MO theory, occupied and vacant MOs can be visualized as being ordered in layers from the lowest to the highest energy eigenvalue. The set of these eigenvalues has upper and lower bounds. The upper energy bound is simply the energy at the end of the quantum states and the beginning of the energy continuum. The lower bound, and for a specific molecule, lies somewhere below the negative of the highest ionization potential of the atoms constituting it (in molecules electrons are less attracted by their own nucleus due to the presence of the remaining nuclei). In the case of bigger and bigger molecules, the number of levels tends to infinity; groups of MOs become very similar in energy over a certain range and form almost continuous bands [64]. But MOs interact electrostatically with one another, trying to minimize their repulsion. Therefore in the case, for example, of exchange of a hydrogen atom for fluorine, we are adding molecular orbitals with energies that should lie between these bounds. These new MOs may change the ordering of the layer and/or the localization of the MOs. Figs. 9-11 show, respectively, the HOMO of molecules 9, 5 and 26 (see Table 4).

We can see that the HOMO is of π nature in all molecules and localized on rings A, B and C. The substituents alter the localization of the HOMO on specific atoms. Note, for example, that the HOMO is not localized on atom 8 (See Fig. 2) in molecule 9, while it is in the case of molecule 5. These differences in the localization of a frontier MO should provide the basis for a fine explanation of, for example, a π-π stacking interaction and/or the electron donating properties of a given atom.

We can see that in molecules 1 and 13 the local (LUMO+1)* of atom 19 has π nature but that the localization on atom 9 is different. In molecule 2 the local (LUMO+1)* of atom 9 has σ nature and therefore it does not participate in charge acceptance. All these differences in localization, magnitude of the localization and nature of the MOs are represented mathematically by the local atomic reactivity indices used here [27]. It is then not extraordinary that, aside from the drug-partner interaction, any measured biological activity should be a linear function of these reactivity indices. Even the hydrophobic properties of a

molecular system can be appropriately accounted for by, for example, the local atomic hardness (and maybe by the local atomic charge capacity).

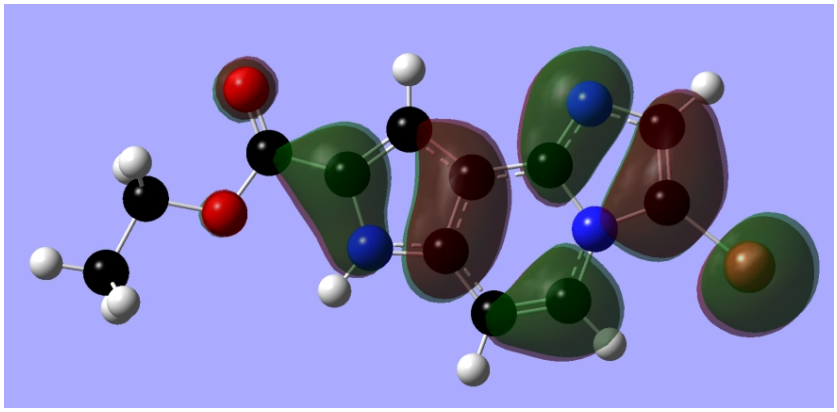

i

Fig. 9. Localization of the highest occupied molecular orbital (HOMO) of molecule 9 (isovalue = 0.02)

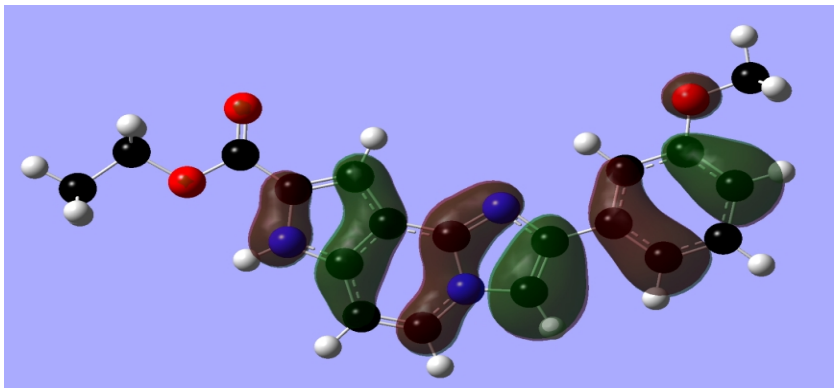

Fig. 10. Localization of the highest occupied molecular orbital (HOMO) of molecule 5 (isovalue = 0.02)

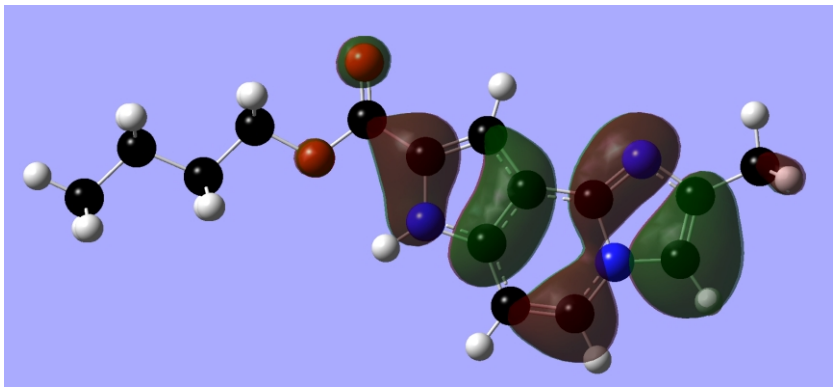

Fig. 11. Localization of the highest occupied molecular orbital (HOMO) of molecule 26 (isovalue = 0.02)

Fig. 12 depicts the LUMO of molecule 3. This MO is almost identical in all molecules of the set analyzed.

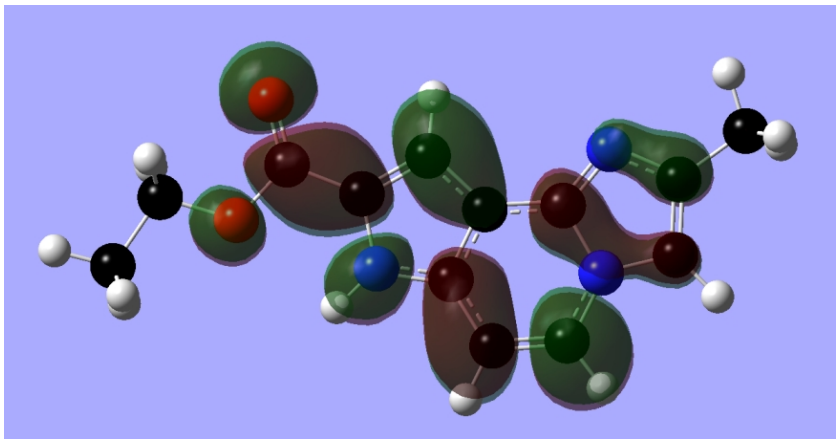

Fig. 12. Localization of the lowest vacant molecular orbital (LUMO) of molecule 3 (isovalue = 0.02)

The magnitude of the localization and the nature of the local MOs can be very different. For example Figs. 13 to 15 show, respectively, the local (LUMO+1)* of atom 9 (see Fig. 2) of molecules 1, 2 and 13.

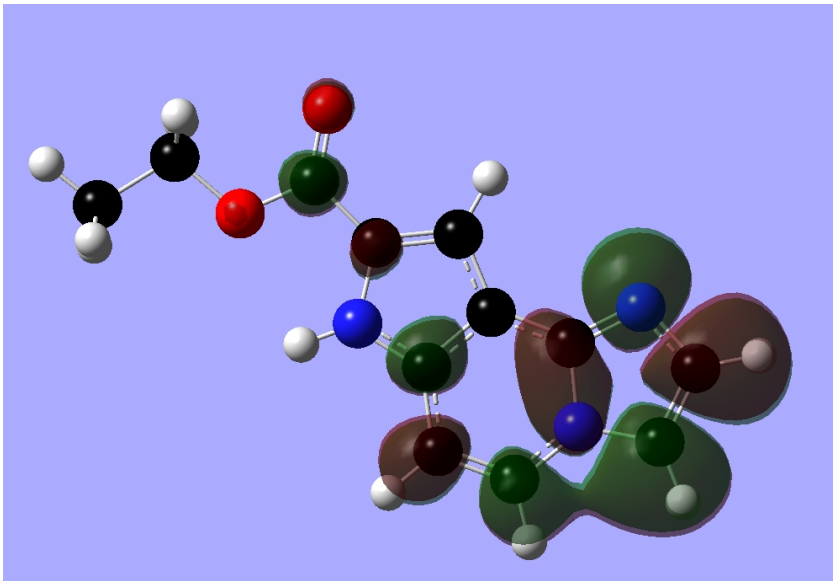

Fig. 13. Localization of the local (LUMO+1)* of atom 9 in molecule 1 (isovalue = 0.02)

The low explanatory ability (by our own standards) of this equation deserves some words. As we said above, the conditions to use a given set of experimental values is that they must have been obtained in nearly identical laboratory conditions and that the action mechanism or mechanisms should be the same for all molecules. Our results strongly suggest that the

set of molecules analyzed here act through different mechanisms. This statement is supported by the impossibility to obtain a statistically significant equation for the whole set of experimental values. Moreover for the potency range 21.8-78.9μM (n=8) no statistically significant results were obtained. This suggests that at high concentrations there is more than one antiviral mechanism. In contrast, a statistically significant equation was obtained for the molecules in the 0.4-47.6 μM range. Fig. 3 shows that several points lie outside the 95% confidence limit. One possible explanation is that the common skeleton hypothesis does not work very well for this case. We think that this possibility can be ruled out because there is no way to include more atoms in this skeleton save the C(O)O group at C9, whose inclusion failed to provide statistically meaningful results. Another possible explanation is that we might be in the presence of extra interactions through the substituents of the common skeleton. A third possibility is related to the range used for obtaining Eq. 4 (0.4-47.6μM). Perhaps there is not a single range, but two different sets of molecules acting in different ways over the whole measured range. To provide a definitive answer we need to wait for a larger set of similar molecules with different substituents at different positions. Note that we found similar dispersions of points in the analysis of indole-based reversible inhibitors of Hepatitis C virus NS5B polymerase [54] and the antiproliferative activity of 1-azabenzanthrone derivatives in normal human fibroblasts [25]. Recently, for a series of (*Z*)-1-aryl-3-arylamino-2-propen-1-ones, we found an equation explaining only 69% of the variation of toxicity against the K562 cell line [57]. Nevertheless, and considering all the approximations made to obtain Eq. 1, the results presented and discussed here indicate that the method employed is suitable for providing a first insight into the molecular action mechanism of these systems. It is possible to speculate that the molecules studied here target the finger domain of the RdRp only because it was shown that similar molecules acted in that way. Unhappily, the method employed here is not able to provide information about what is the exact location at which the molecules studied here bind. Nevertheless we may state the following general rule: any result obtained for the molecules analyzed in this paper with other methods (molecular modeling or docking) must be fully compatible with the results presented here.

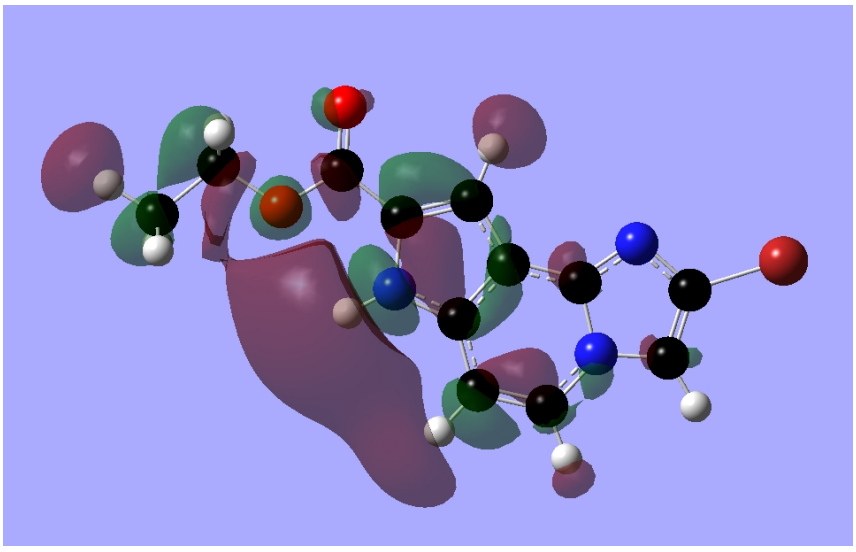

Fig. 14. Localization of the local (LUMO+1)* of atom 9 in molecule 2 (isovalue = 0.02).

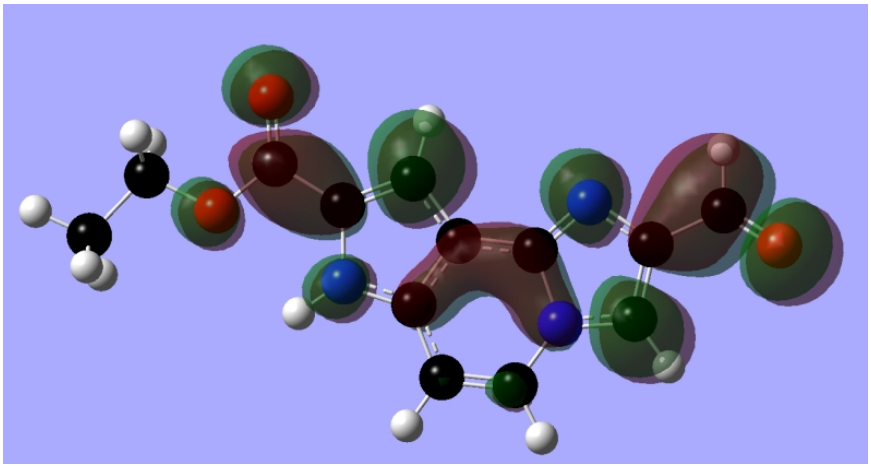

Fig. 15. Localization of the local (LUMO+1)* of atom 9 in molecule 13 (isovalue = 0.02)

4. CONCLUSION

We have obtained statistically significant results relating the variation of a definite set of local atomic reactivity indices to the variation of antiviral activity against the Bovine Viral Diarrhea Virus for a series of imidazo [1,2-*a*] pyrrolo [2,3-*c*] pyridine derivatives. The whole process is orbital-controlled. The results suggest that the subset of molecules with highest antiviral activity seems to have a different action mechanism than molecules with low activity. The exact boundary between the two sets could not be defined clearly. More experimental information is needed to clarify this point.

ACKNOWLEDGEMENTS

Prof. Dr. Bruce K. Cassels (Faculty of Sciences, University of Chile) is gratefully acknowledged for helpful comments. This paper is dedicated to the late Dr. Federico Peradejordi (Centre de Mécanique Ondulatorie Appliqueé du CNRS, Paris, France) who taught me the first concepts of quantum pharmacology.

COMPETING INTERESTS

The author declares that no competing interests exist.

REFERENCES

1. Xia H, Liu L, Wahlberg N, Baule C, Belák S. Molecular phylogenetic analysis of bovine viral diarrhoea virus: A Bayesian approach, Virus Res. 2007;130:53-62.
2. Ridpath JF. Bovine Viral Diarrhea Virus, in Encyclopedia of Virology (Third Edition), Mahy BWJ, Regenmortel MHVV. Eds. Academic Press, Oxford. 2008;374-380.
3. Neill JD, Molecular biology of bovine viral diarrhea virus, Biologicals. 2013;41:2-7.
4. Tao J, Liao J, Wang Y, Zhang X, Wang J, Zhu G. Bovine viral diarrhea virus (BVDV) infections in pigs, Vet. Microbiol. 2013;165:185-189.

5. Kozasa T, Tajima M, Yasutomi I, Sano K, Ohashi K, Onuma M. Relationship of bovine viral diarrhea virus persistent infection to incidence of diseases on dairy farms based on bulk tank milk test by RT-PCR, Vet. Microbiol. 2005;106:41-47.
6. Lindberg A, Houe H, Characteristics in the epidemiology of bovine viral diarrhea virus (BVDV) of relevance to control, Prev. Vet. Med. 2005;72:55-73.
7. Valle PS, Skjerve E, Martin SW, Larssen RB, Østerås O, Nyberg O. Ten years of bovine virus diarrhoea virus (BVDV) control in Norway: a cost-benefit analysis, Prev. Vet. Med. 2005;72:189-207.
8. Gard JA, Givens, MD, Stringfellow, DA, Bovine viral diarrhea virus (BVDV): Epidemiologic concerns relative to semen and embryos, Theriogen. 2007;68:434-442.
9. Heuer C, Healy A, Zerbini C, Economic Effects of Exposure to Bovine Viral Diarrhea Virus on Dairy Herds in New Zealand, J. Dayr. Sci. 2007;90:5428-5438.
10. Kim SG, Anderson RR, Yu,JZ, Zylich NC, Kinde H, Carman S, Bedenice D, Dubovi, EJ. Genotyping and phylogenetic analysis of bovine viral diarrhea virus isolates from BVDV infected alpacas in North America, Vet. Microbiol. 2009;136:209-216.
11. Ridpath JF. Bovine Viral Diarrhea Virus: Global Status, Vet. Clin. North Am. Food. An. Pract. 2010;26:105-121.
12. Friedgut O, Rotenberg D, Brenner J, Yehuda S, Paz R, Alpert N, Ram A, Yadin H, Grummer B. Description of the first acute bovine diarrhea virus-2 outbreak in Israel, Vet. J. 2011;189:108-110.
13. Luzzago C, Ebranati E, Sassera D, Lo Presti A, Lauzi S, Gabanelli E, Ciccozzi M, Zehender G. Spatial and temporal reconstruction of bovine viral diarrhea virus genotype 1 dispersion in Italy, Infect. Genet. Evol. 2012;12:324-331.
14. Kuta A, Polak MP, Larska M, Żmudziński JF. Predominance of bovine viral diarrhea virus 1b and 1d subtypes during eight years of survey in Poland, Vet. Microbiol. 2013;166:639-644.
15. Atherton MJ, Lichty BD. Evolution of oncolytic viruses: novel strategies for cancer treatment, Immunotherapy. 2013;5:1191-1206.
16. Choi KH, Groarke JM, Young DC, Kuhn RJ, Smith JL, Pevear DC, Rossmann MG. The structure of the RNA-dependent RNA polymerase from bovine viral diarrhea virus establishes the role of GTP in de novo initiation, Proceedings of the National Academy of Sciences of the United States of America. 2004;101:4425-4430.
17. Paeshuyse J, Leyssen P, Mabery E, Boddeker N, Vrancken R, Froeyen M, Ansari IH, Dutartre H, Rozenski J, Gil LHVG, Letellier C, Lanford R, Canard B, Koenen F, Kerkhofs P, Donis RO, Herdewijn P, Watson J, De Clercq E, Puerstinger G, Neyts J. A Novel, Highly Selective Inhibitor of Pestivirus Replication That Targets the Viral RNA-Dependent RNA Polymerase, Journal of Virology. 2006;80:149-160.
18. Chezal J-M, Paeshuyse J, Gaumet V, Canitrot D, Maisonial A, Lartigue C, Gueiffier A, Moreau E, Teulade J-C, Chavignon O, Neyts J. Synthesis and antiviral activity of an imidazo [1,2-a] pyrrolo [2,3-c] pyridine series against the bovine viral diarrhea virus, Eur. J. Med. Chem. 2010;45:2044-2047.
19. Gómez-Jeria JS. On some problems in quantum pharmacology I. The partition functions, Int. J. Quant. Chem. 1983;23:1969-1972.
20. Gómez-Jeria JS. Modeling the Drug-Receptor Interaction in Quantum Pharmacology. in Molecules in Physics, Chemistry, and Biology. J. Maruani Ed., Springer Netherlands. 1989;4:215-231.
21. Gómez-Jeria JS, Ojeda-Vergara, M, Donoso-Espinoza, C, Quantum-chemical Structure-Activity Relationships in carbamate insecticides, Mol. Engn. 1995;5:391-401.
22. Gómez-Jeria, JS, Ojeda-Vergara, M, Parametrization of the orientational effects in the drug-receptor interaction, J. Chil. Chem. Soc. 2003;48:119-124.

23. Bruna-Larenas T, Gómez-Jeria JS. A DFT and Semiempirical Model-Based Study of Opioid Receptor Affinity and Selectivity in a Group of Molecules with a Morphine Structural Core, Int. J. Med. Chem. 2012;(Article ID)682495:1-16.
24. Gómez-Jeria JS, Elements of Molecular Electronic Pharmacology (In Spanish), Ediciones Sokar, Santiago de Chile; 2013.
25. Gómez-Jeria JS, Flores-Catalán M, Quantum-chemical modeling of the relationships between molecular structure and in vitro multi-step, multimechanistic drug effects. HIV-1 replication inhibition and inhibition of cell proliferation as examples., Canad. Chem. Trans. 2013;1:215-237.
26. Fukui K, Fujimoto H. Frontier orbitals and reaction paths*:* Selected papers of Kenichi Fukui, World Scientific, Singapore; River Edge, N.J.; 1997.
27. Gómez-Jeria JS. A New Set of Local Reactivity Indices within the Hartree-Fock-Roothaan and Density Functional Theory Frameworks, Canad. Chem. Trans. 2013;1:25-55.
28. Mulliken RS. Electronic Population Analysis on LCAO–MO Molecular Wave Functions. I, J. Chem. Phys. 1955;23:1833-1840.
29. Gómez-Jeria JS. Espinoza, L, Estudios químico-cuánticos de la inhibición de la acetilcolinesterasa. I. Carbamatos, Bol. Soc. Chil. Quím. 1982;27:142-144.
30. Gómez-Jeria JS, Morales-Lagos D. The mode of binding of phenylalkylamines to the Serotonergic Receptor, in QSAR in design of Bioactive Drugs, M. Kuchar Ed., Prous, J.R., Barcelona, Spain. 1984;145-173.
31. Gómez-Jeria JS, Morales-Lagos DR, Quantum chemical approach to the relationship between molecular structure and serotonin receptor binding affinity, J. Pharm. Sci. 1984;73:1725-1728.
32. Gómez-Jeria JS, Morales-Lagos D, Rodriguez-Gatica JI, Saavedra-Aguilar JC. Quantum-chemical study of the relation between electronic structure and pA2 in a series of 5-substituted tryptamines, Int. J. Quant. Chem. 1985;28:421-428.
33. Gómez-Jeria JS, Morales-Lagos D, Cassels BK, Saavedra-Aguilar JC. Electronic structure and serotonin receptor binding affinity of 7-substituted tryptamines QSAR of 7-substituted tryptamines, Quant. Struct.-Relat. 1986;5:153-157.
34. Gómez-Jeria JS, Sotomayor P. Quantum chemical study of electronic structure and receptor binding in opiates, J. Mol. Struct. (Theochem). 1988;166:493-498.
35. Gómez-Jeria JS, Lagos-Arancibia, L, Quantum-chemical structure-affinity studies on kynurenic acid derivatives as Gly/NMDA receptor ligands, Int. J. Quant. Chem. 1999;71:505-511.
36. Gómez-Jeria JS, Lagos-Arancibia L, Sobarzo-Sánchez E. Theoretical study of the opioid receptor selectivity of some 7-arylidenenaltrexones, Bol. Soc. Chil. Quím., 2003;48:61-66.
37. Gómez-Jeria JS, Soto-Morales F, Larenas-Gutierrez G. A Zindo/1 Study of the Cannabinoid-Mediated Inhibition of Adenylyl Cyclase, Ir. Int. J. Sci. 2003;4:151-164.
38. Gómez-Jeria JS, Gerli-Candia LA, Hurtado SM. A structure-affinity study of the opioid binding of some 3-substituted morphinans, J. Chil. Chem. Soc. 2004;49:307-312.
39. Soto-Morales F, Gómez-Jeria JS. A theoretical study of the inhibition of wild-type and drug-resistant HTV-1 reverse transcriptase by some thiazolidenebenzenesulfonamide derivatives, J. Chil. Chem. Soc. 2007;52:1214-1219.
40. Gómez-Jeria JS, Soto-Morales F, Rivas J, Sotomayor A. A theoretical structure-affinity relationship study of some cannabinoid derivatives, J. Chil. Chem. Soc. 2008;53:1393-1399.

41. Gómez-Jeria JS. A DFT study of the relationships between electronic structure and peripheral benzodiazepine receptor affinity in a group of N,N-dialkyl-2- phenylindol-3-ylglyoxylamides (Erratum in: J. Chil. Chem. Soc., 55, 4, IX, 2010), J. Chil. Chem. Soc. 2010;55:381-384.
42. Gómez-Jeria JS. A quantum-chemical analysis of the relationships between hCB2 cannabinoid receptor binding affinity and electronic structure in a family of 4-oxo-1,4-dihydroquinoline-3-carboxamide derivatives, Der Pharmacia Lettre. 2014;6:95-104.
43. Salgado-Valdés F, Gómez-Jeria JS. A Theoretical Study of the Relationships between Electronic Structure and CB1 and CB2 Cannabinoid Receptor Binding Affinity in a Group of 1-Aryl-5-(1-H-pyrrol-1-yl)-1-H-pyrazole-3-carboxamides, J. Quant. Chem., 2014;(Article ID)431432:1-15.
44. Agin D, Hersh L, Holtzman D. The action of anesthetics on excitable membranes: a quantum-chemical analysis, Proc. Natl. Acad. Sci. (USA). 1965;53:952-958.
45. Hudson RF, Klopman G. A general perturbation treatment of chemical reactivity, Tet. Lett. 1967;8:1103-1108.
46. Klopman G, Hudson RF. Polyelectronic perturbation treatment of chemical reactivity, Theoret. Chim. Acta. 1967;8:165-174.
47. Cammarata A. Some electronic factors in drug-receptor interactions, J. Med. Chem. 1968;11:1111-1115.
48. Cammarata A, Stein RL. Molecular orbital methods in the study of cholinesterase inhibitors, J. Med. Chem. 1968;11:829-833.
49. Klopman G, Chemical reactivity and the concept of charge- and frontier-controlled reactions, J. Am. Chem. Soc. 1968;90:223-234.
50. Peradejordi F, Martin AN, Cammarata A. Quantum chemical approach to structure-activity relationships of tetracycline antibiotics, J. Pharm. Sci. 1971;60:576-582.
51. Gómez-Jeria JS. Calculation of the nucleophilic superdelocalizability by the CNDO/2 method, J. Pharm. Sci. 1982;71:1423-1424.
52. Barahona-Urbina C, Nuñez-Gonzalez S, Gómez-Jeria JS. Model-based quantum-chemical study of the uptake of some polychlorinated pollutant compounds by Zucchini subspecies, J. Chil. Chem. Soc. 2012;57:1497-1503.
53. Alarcón DA, Gatica-Díaz F, Gómez-Jeria JS. Modeling the relationships between molecular structure and inhibition of virus-induced cytopathic efects. Anti-HIV and anti-H1N1 (Influenza) activities as examples, J. Chil. Chem. Soc. 2013;58:1651-1659.
54. Paz de la Vega A, Alarcón DA, Gómez-Jeria JS. Quantum Chemical Study of the Relationships between Electronic Structure and Pharmacokinetic Profile, Inhibitory Strength toward Hepatitis C virus NS5B Polymerase and HCV replicons of indole-based compounds., J. Chil. Chem. Soc. 2013;58:1842-1851.
55. Reyes-Díaz I, Gómez-Jeria JS. Quantum-chemical modeling of the hepatitis C virus replicon inhibitory potency and cytotoxicity of some pyrido [2,3-d] pyrimidine analogues, J. Comput. Methods Drug Des. 2013;3:11-21.
56. Gómez-Jeria JS. A theoretical study of the relationships between electronic structure and anti-inflammatory and anti-cancer activities of a series of 6,7-substituted-5,8-quinolinequinones, Int. Res. J. Pure App. Chem. 2014;4:270-291.
57. Pino-Ramírez DI, Gómez-Jeria JS. A Quantum-chemical study of the in vitro cytotoxicity of a series of (Z)-1-aryl-3-arylamino-2-propen-1-ones against human tumor DU145 and K562 cell lines, American Chemical Science, in press; 2014.
58. Frisch MJ, Trucks GW, Schlegel HB, Scuseria GE, Robb MA, Cheeseman JR, Montgomery J, JA, Vreven T, Kudin KN, Burant JC, Millam JM, Iyengar SS, Tomasi J, Barone V, Mennucci B, Cossi M, Scalmani G, Rega N. Gaussian98 Rev. A.11.3, Gaussian, Pittsburgh, PA, USA; 2002.

59. Gómez-Jeria JS, An empirical way to correct some drawbacks of Mulliken Population Analysis (Erratum in: J. Chil. Chem. Soc., 55, 4, IX, 2010), J. Chil. Chem. Soc. 2009;54:482-485.
60. Statsoft, Statistica 8.0, 2300 East 14 th St. Tulsa, OK 74104, USA; 1984-2007.
61. Ariens EJ, Molecular pharmacology*:* The mode of action of biologically active compounds, edited by E.J. Ariens*,* Academic Press, New York; 1964.
62. Dennington, RD, Keith, TA, Millam, JM, GaussViev 5.0.8, 340 Quinnipiac St., Bldg. 40, Wallingford, CT 06492, USA; 2000-2008.
63. Varetto U. Molekel 5.4.0.8, Swiss National Supercomputing Centre: Lugano, Switzerland; 2008.
64. Gómez-Jeria JS. Minimal molecular models for the study of nanostructures, J. Comp. Theor.Nanosci. 2009;6:1361-1369.

Peer-review history:
The peer review history for this paper can be accessed here:
http://www.sciencedomain.org/review-history.php?iid=525&id=8&aid=4645